Analysis of Fracture Toughness in the Transition Temperature Region of API X70 Pipeline Steels Rolled in Two-Phase Region

SANG YONG SHIN, GUILIANG GONG, SANGHO KIM, and SUNGHAK LEE

In this study, fracture toughness in the transition temperature region of three API X70 line pipe steels rolled in the two-phase ($\alpha + \gamma$) region was analyzed in accordance with the ASTM E1921-05 standard test method. Elastic-plastic cleavage fracture toughness (K_{Jc}) was determined by three-point bend tests, using precracked Charpy V-notch specimens, and then the measured K_{Jc} values were interpreted by the three-parameter Weibull distribution. The fracture toughness test results indicated that the master curve and the 98 pct confidence curves explained the variation in the measured fracture toughness values well. Reference temperatures obtained from the fracture toughness tests as well as index temperatures obtained from the Charpy impact tests were lowest in the steel cooled at 500 °C, which did not contain brittle martensite and had a small effective grain size. In this steel, the absence of martensite led to the higher resistance to cleavage crack initiation, and the smaller effective grain size led to the higher possibility of crack arrest, thereby resulting in the best overall fracture properties.

DOI: 10.1007/s11661-007-9125-6

I. INTRODUCTION

RECENTLY produced line pipe steels contribute greatly to energy conservation, cost reduction, and improved transportation efficiency, because they allow long-distance transportation of a large amount of crude oil or natural gas under high pressure.[1,2,3] They have become stronger, tougher, thicker, and larger because the gas composition has become richer and many drilling activities have been undertaken in severe conditions such as extremely cold or deep regions.

As high strength is generally achieved at the expense of reduced toughness and ductility, it is imperative to scrutinize the structural integrity related to low-temperature toughness in order to safely manage line pipe steels at extremely cold or deep regions. To evaluate fracture properties of line pipe steels, various laboratory-scale testing methods, which correspond closely to the full-scale fracture behavior, have been studied.[4,5,6] Among them, the Charpy V-notch impact test and drop-weight tear test (DWTT) are most widely used.[1–5,7] However, these tests are not based on fracture mechanics to evaluate fracture toughness, and their data may have large deviations in the transition temperature region because they largely depend on specimen size and geometry. Furthermore, contrary to the values obtained from fracture toughness tests in accordance with ASTM standards, those measured from the Charpy impact test and DWTT are not transferable to structural components. In order to quantitatively evaluate fracture toughness and its distribution, advanced standard testing methods based on the probabilistic and statistical analysis of fracture mechanics are needed. Recently, the American Society for Testing Materials (ASTM) suggested the ASTM E1921-05 standard test method,[8] in which the variation of fracture toughness in the transition temperature region is considered as a property of ferritic steels. According to this test method, variations in fracture toughness as a function of temperature can be explained using a master curve characterized by a reference temperature.

In the present study, fracture toughness in the transition temperature region of three kinds of API X70 line pipe steels rolled in the two-phase ($\alpha + \gamma$) region was analyzed in accordance with the ASTM E1921-05 standard test method.[8] The reference temperature, which characterizes fracture toughness in the transition region, was compared with the index temperatures obtained from the Charpy impact test, based on which microstructural factors affecting fracture toughness were investigated.

II. EXPERIMENTAL

A. *Materials*

An API X70 grade steel having a yield strength level of 483 MPa (70 ksi) was used; its chemical composition was Fe-0.05C-0.27Si-1.24Mn-0.22Cu-0.19Ni-0.08Mo-0.1(Nb + V + Ti) (wt pct). Overall grain refinement was expected by rolling with a high rolling reduction

SANG YONG SHIN, Research Assistant, is with the Center for Advanced Aerospace Materials, Pohang University of Science and Technology, Pohang 790-784, Korea. GUILIANG GONG, Engineer, is with Cold Rolling Mill Technology–Quality Control Department, Wu Han Iron and Steel Processing Corporation, Ltd., Hu Bei Province 430083, China. SANGHO KIM, Principal Researcher, is with the Plate Research Group, Technical Research Laboratories, POSCO, Pohang 790-785, Korea. SUNGHAK LEE, Professor, is with the Center for Advanced Aerospace Materials and the Materials Science and Engineering Department, Pohang University of Science and Technology. Contact e-mail: shlee@postech.ac.kr

Manuscript submitted February 8, 2006.
Article published online May 8, 2007.

Table I. Rolling Conditions of the API X70 Steel Steels

Steel	Reheating Temp. (°C)	Start Rolling Temp. (°C)	Finish Rolling Temp. (°C)	Start Cooling Temp. (°C)	Finish Cooling Temp. (°C)	Cooling Rate (°C/s)
T4	1200	910	below Ar_3	below Ar_3	400	11 to 14
T5					500	10 to 12
T6					600	5 to 9

ratio of 75 pct in the nonrecrystallized region of austenite after austenitization at 1200 °C.[9,10,11] Rolling was finished in the two-phase region below Ar_3. The Ar_3 is the temperature at which proeutectoid ferrite starts to form from austenite during cooling. After the finish rolling, the steels were cooled rapidly to a finish cooling temperature (FCT) of 400 °C, 500 °C, or 600 °C. The rolling conditions are shown in Table I. For convenience, the steels rolled in the two-phase region and cooled to 400 °C, 500 °C, and 600 °C are referred to as "T4," "T5," or "T6," respectively (Table I).

B. *Microstructural Analysis*

The longitudinal-transverse (L-T) and longitudinal-short transverse (L-S) planes of the rolled steels were polished and etched by a 2 pct nital solution, and microstructures were observed by an optical microscope and a scanning electron microscope (SEM). The volume fraction of martensite or bainite present in the steels was measured in an image analyzer. Electron backscatter diffraction (EBSD) analysis[12] was conducted on the rolled steels with a field emission–scanning electron microscope (FE-SEM, model: S-4300SE, Hitachi, Tokyo, Japan, resolution: 0.2 μm). The data were then interpreted by orientation imaging microscopy analysis software provided by TexSEM Laboratories, Inc. Provo, UR, USA.

C. *Tensile and Charpy Impact Tests*

Round tensile specimens with a gage diameter of 6 mm and a gage length of 30 mm were prepared in the transverse direction and were tested at room temperature at a crosshead speed of 5 mm/min using an Instron machine of 100 kN capacity. Low-temperature tensile tests were conducted in the temperature range from −140 °C to 20 °C after the tensile specimens were kept for 15 minutes inside a low-temperature chamber in which the test temperature was controlled by spraying liquid nitrogen. Charpy impact tests were performed on standard Charpy V-notch specimens (size: $10 \times 10 \times 55$ mm, orientation; transverse-longitudinal (T-L)) in the temperature range from −196 °C to 20 °C using a Tinius Olsen impact tester of 500 J capacity (Model: FAHC-J-500-01, JT Toshi, Tokyo, Japan).[13] In order to reduce errors in the data interpretation, a regression analysis for absorbed impact energy *vs* test temperature was conducted with a hyperbolic tangent curve fitting method.[14] Based on the regression analysis data, various index temperatures such as T_{28J}, T_{41J}, and T_{68J} were obtained, and the energy transition temperature (ETT), which corresponds to the average value of upper-shelf energy (USE) and lower-shelf energy (LSE), was determined as well. The T_{28J}, T_{41J}, and T_{68J} are temperatures at which the absorbed impact energy values are 28, 41, and 68 J, respectively.

D. *Fracture Toughness Test*

Fracture toughness in the transition temperature region was analyzed in accordance with the ASTM E1921-05 standard test method.[8] Three-point bending tests were conducted on precracked Charpy V-notch (PCVN) specimens with the T-L orientation whose initial crack length was about 5 mm. Fatigue precracking was done under a stress ratio, R, controlled within the range of $0.01 < R < 0.1$. The test temperature was fixed at −120 °C and −100 °C, which were lower than the T_{28J} of the three rolled steels, in accordance with the ASTM E1921-05 standard specification,[8] and was controlled within ±0.5 °C by liquid nitrogen in a low-temperature chamber filled with isopentane. Load was applied to a PCVN specimen until unstable brittle fracture occurred in the transition region in order to obtain J_c, which was then converted to K_{Jc}:

$$K_{Jc} = \sqrt{J_c \cdot E/(1 - \nu^2)} \qquad [1]$$

where E is the elastic modulus. The measured K_{Jc} was used after checking if it met the following condition:

$$K_{Jc} \leq \{Eb_0\sigma_{ys}/30(1 - \nu^2)\}^{1/2} \qquad [2]$$

where b_0 and σ_{ys} are the initial ligament and yield strength at the test temperature, respectively.

When the number of valid K_{Jc} data measured at the same test temperature is more than six, the reference temperature (T_o) was determined in the following way. First, the K_{Jc} values obtained from each specimen were converted to fracture toughness values corresponding to 1-in. size specimen, $K_{Jc(1T)}$:

$$K_{Jc(1T)} = K_{\min} + [K_{Jc} - K_{\min}]\left(\frac{B}{B_{(1T)}}\right)^{1/4} \qquad [3]$$

where $K_{\min}$ is 20 MPa $m^{1/2}$, B is the actual specimen thickness, and $B_{(1T)}$ refers to 1 in. The maximum likelihood method was applied to the $K_{Jc(1T)}$ data in

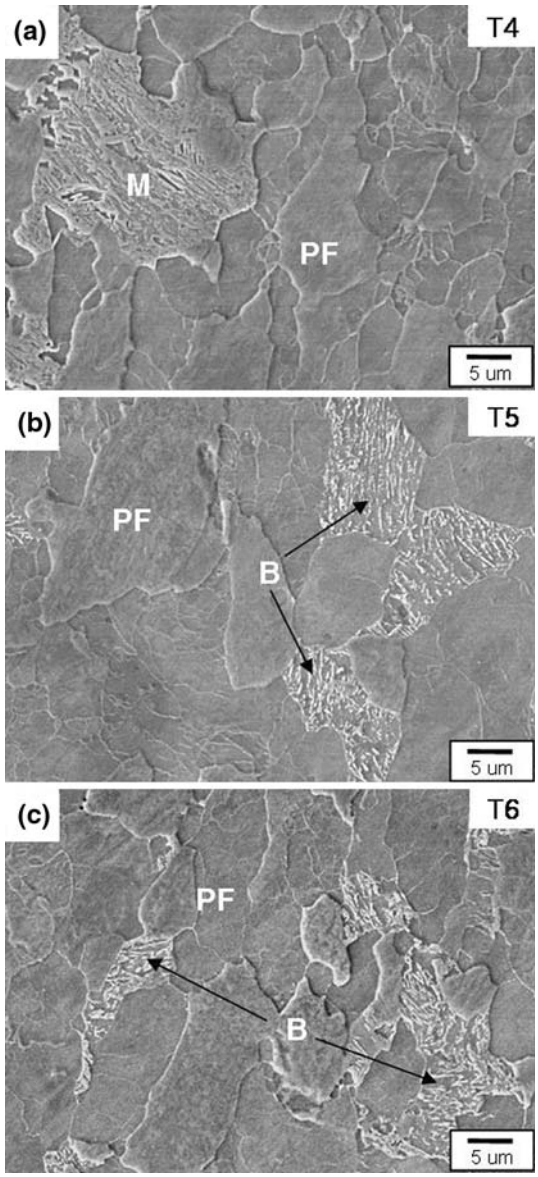

Fig. 1—SEM micrographs of the (*a*) T4, (*b*) T5, and (*c*) T6 steels (L-T plane). Nital etched.

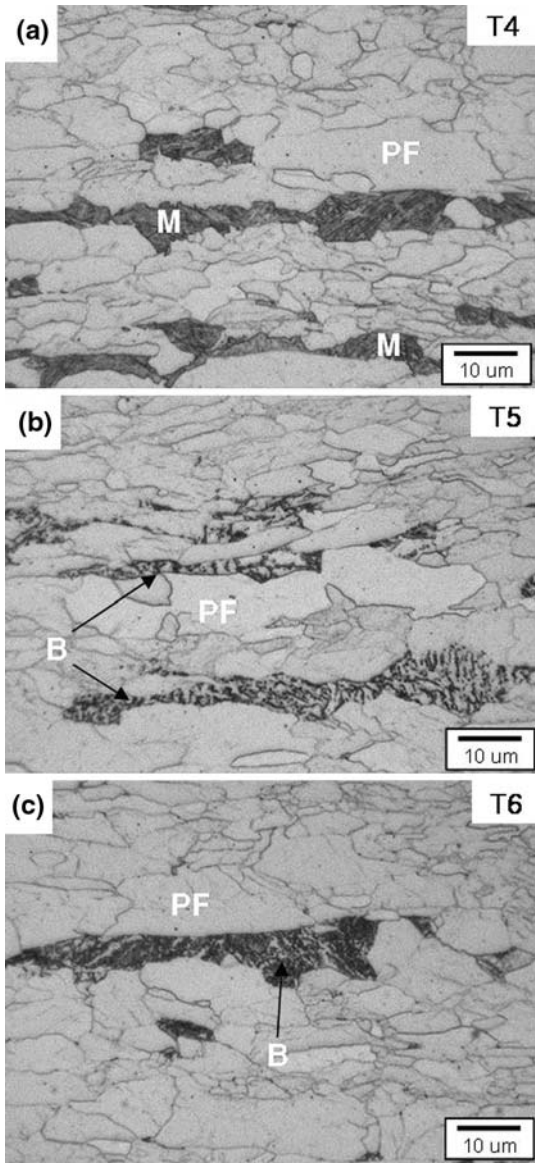

Fig. 2—Optical micrographs of the (*a*) T4, (*b*) T5, and (*c*) T6 steels (L-S plane). Nital etched.

order to determine the scale parameter (K_o), and $K_{Jc(\text{med})}$ that corresponds to the 50 pct cumulative fracture probability was calculated by the following equation:

$$K_{Jc(\text{med})} = (K_o - K_{\min})[\ln\ (2)]^{1/4} + K_{\min} \qquad [4]$$

The reference temperature (T_o) whose $K_{Jc(\text{med})}$ value is 100 MPa $\text{m}^{1/2}$ for the $1T$ specimen was determined by the equation

$$T_o = T - \frac{1}{0.019}\ln\left(\frac{K_{Jc(\text{med})} - 30}{70}\right) \qquad [5]$$

where T is the test temperature.

III. RESULTS

A. *Microstructure*

Figures 1(a) through (c) are SEM micrographs of the L-T plane of the API X70 steels. The three steels rolled in the two-phase region consist mainly of polygonal ferrite (PF) transformed before or during finish rolling, together with a small amount of martensite or bainite. Microhardness of ferrite, bainite, and martensite was measured by an ultra-micro-Vickers hardness tester under a load of 5 g, and the hardness results are 201, 298, and 337 VHN, respectively. The volume fraction of martensite present in the T4 steel is 6.3 pct, while the volume fractions of bainite present in the T5 and T6 steels are 5.6 and 2.4 pct, respectively. Optical micrographs of the L-S plane are shown in Figures 2(a) through (c). A band structure is clearly observed as

some PF grains formed at austenite grain boundaries were elongated during rolling.[9]

The results of the EBSD analysis of the three steels are provided in Figures 3(a) through (c). These grain-color maps can be represented in different colors, depending on the orientation of each point. If a certain misorientation is designated, points that are smaller than the designated misorientation can be colored in a single color. The boundaries between grains having different orientations of 15 deg or higher are high-angle boundaries. These grains are generally considered to be effective ones, which can play a role in crack arrest, because the smaller effective grain size leads to the higher possibility of crack arrest.[15,16,17] The effective grain sizes of the T4, T5, and T6 steels were measured to be 7.6, 9.1, and 12.1 μm, respectively.

B. *Tensile and Charpy Impact Test Results*

Stress-strain curves for the three steels tested at room temperature are shown in Figure 4, from which the results of yield strength, tensile strength, and elongation are obtained, as shown in Table II. Variations of yield and tensile strengths as a function of test temperature are also plotted in Figures 5(a) and (b). Yield and tensile strengths increase as the temperature decreases (Figures 5(a) and (b)). Because the three steels exhibit yield strengths exceeding 483 MPa at room temperature (Table II), all the steels satisfy the strength requirement of X70 grade line pipe steels. The tensile strength of the T4 steel containing martensite in the PF matrix is higher than that of the T6 steel, whereas the elongation is lower. In the T5 and T6 steels containing bainite, the yield and tensile strengths of the T5 steel are higher than those of the T6 steel because of the higher volume fraction of bainite, and the elongation of the T5 steel is higher than that of the T6 steel.[18]

The Charpy impact test results are shown in Figures 6(a) through (d), from which the results of USE, ETT, T_{28J}, T_{41J}, and T_{68J} are obtained, as shown in Table III. The USE is highest in the T5 steel and decreases in the order of the T6 and T4 steels. The three steels exhibit excellent ETT properties (below −80 °C). T_{28J} obtained from the Charpy impact test is −117 °C, −127 °C, and −116 °C for the T4, T5, and T6 steels, respectively. Other index temperatures, T_{41J} and T_{68J}, have similar trends to T_{28J} and are lowest in the T5 steel.

Figures 7(a) through (c) are SEM micrographs of the Charpy impact specimens fractured at −196 °C, showing the cleavage crack propagation path. In the T4 steel containing a lot of fine high-angled PF, the cleavage crack path is changed at PF interfaces (Figure 7(a)), which confirms that the T4 steel has a smaller effective grain size than the other steels. These results of the cleavage crack propagation path match well with the EBSD results of Figures 3(a) through (c).

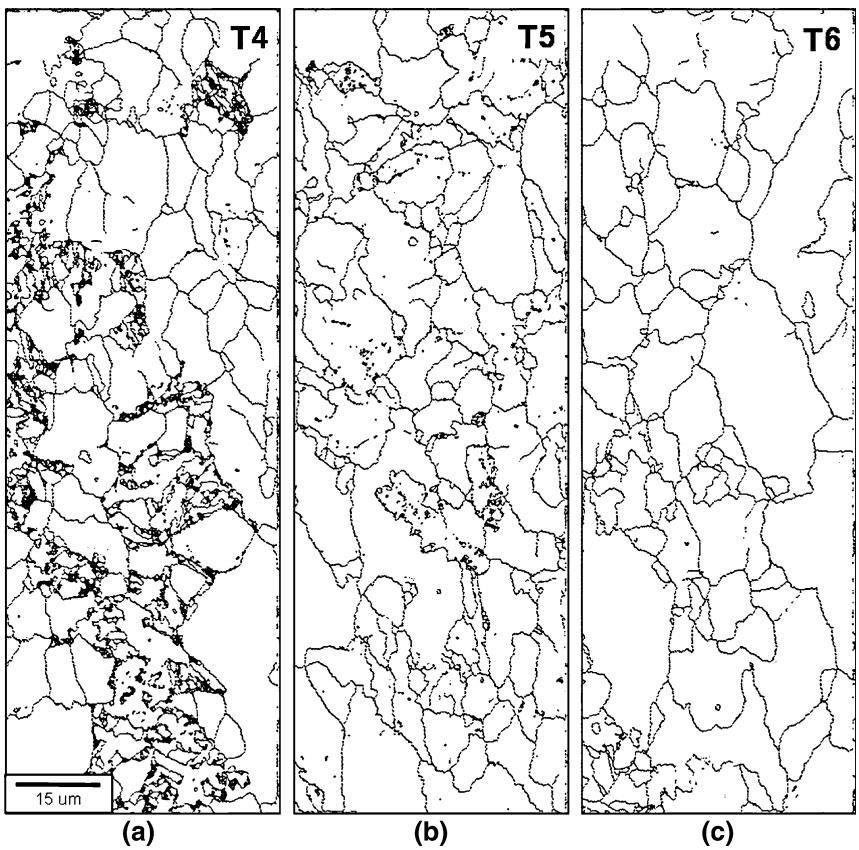

Fig. 3—EBSD crystal orientation maps showing high-angle (≥15 deg) boundaries of the (*a*) T4, (*b*) T5, and (*c*) T6 steels.

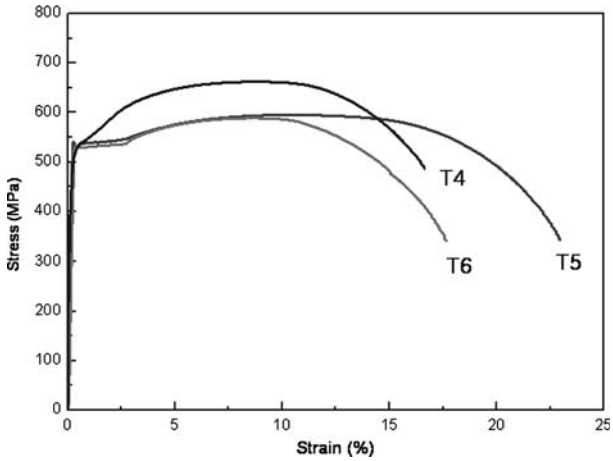

Fig. 4—Stress-strain curves for the three steels tested at room temperature.

Table II. Room-Temperature Tensile Test Results

Steel	Yield Strength (MPa)	Tensile Strength (MPa)	Elongation (Pct)
T4	523	662	17
T5	538	595	23
T6	532	589	18

C. *Fracture Toughness*

The fracture toughness test results reveal cleavage fracture after some plastic deformation at the fatigued precrack tip in the transition temperature region. The reference temperatures (T_o) of the T4, T5, and T6 steels whose $K_{Jc(\text{med})}$ is 100 MPa $m^{1/2}$ for the 1-in.-size specimen were calculated to be −90 °C, −97 °C, and −90 °C, respectively, from the distribution of their fracture toughness values, as shown in Tables IV and V. The revised 2005 version of the ASTM E1921 standard test method was used, because the results obtained from the old versions of the standard were significantly different from those obtained from the revised 2005 version. The master curves determined from the measured reference temperatures, together with the measured values of elastic-plastic cleavage fracture toughness, are presented in Figures 8(a) through (c). The solid line indicates the fracture toughness of 50 pct cumulative fracture probability, while the dotted lines show the region of 98 pct confidence for the presented master curve. It is known from Figures 8(a) through (c) that the scatters of the fracture toughness data are well explained by the master curves and the 98 pct confidence curves.

The uncertainty of T_o can be calculated by the following equation:

$$\Delta T_0 = \frac{\beta}{\sqrt{r}} \cdot Z_{95} \qquad [6]$$

Because the calculated $K_{Jc(\text{med})eq}$ is higher than 82 MPa $m^{1/2}$, β is determined to be 18 °C. The number of effective K_{Jc} data points was 20, 17, and 19 for the T4, T5, and T6 steels, respectively, and the 95 pct confidence was considered. The value of ΔT_o is calculated to be 8 °C, 9 °C, and 8 °C for the T4, T5, and T6 steels, respectively, as shown in Table VI.

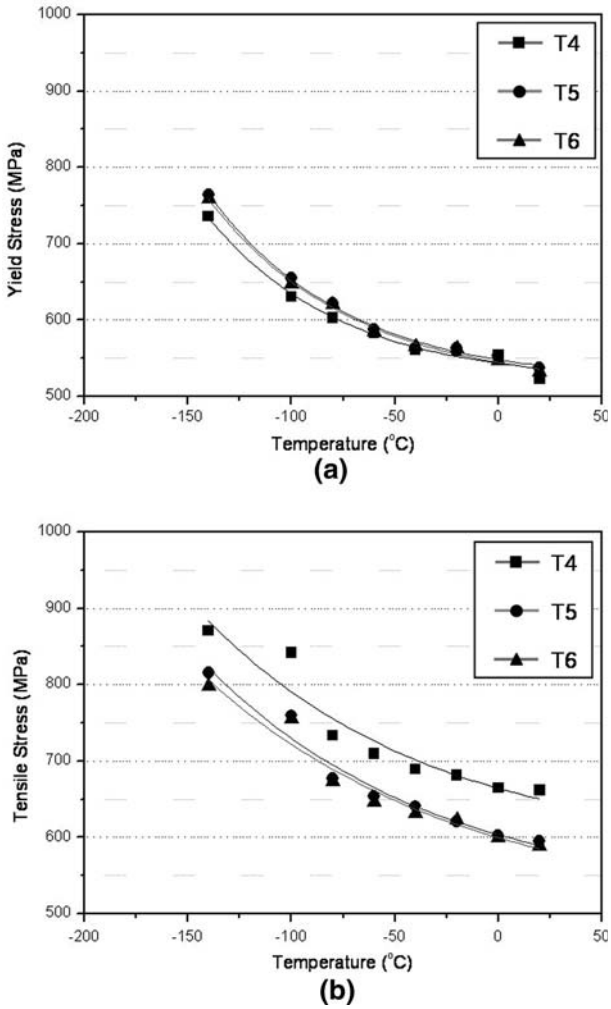

Fig. 5—Variation of (*a*) yield strength and (*b*) tensile strength of the T4, T5, and T6 steels as a function of test temperature.

The expected test temperature can be estimated to be about −170 °C by $T = T_{28J} + (-50\ ^\circ\text{C})$ in accordance with the test temperature selection of the ASTM E1921-05 standard.[8] Because this temperature is included in the LSE range, the test temperature of the present study is determined to be −120 °C and −100 °C, which are higher than −170 °C. Because the calculated T_o ranges from −100 °C to −90 °C, these test temperatures (−120 °C and −100 °C) are reliably included in the temperature range of $T_o \pm 50$ °C.

Weibull plots, which can show whether the measured test data satisfy the Weibull probability distribution, are provided in Figures 9(a) through (c). Weibull slope, m, determined by the linear regression analysis, defines the scatter of the test data on the Weibull distribution. According to Wallin[19] and Anderson *et al.*,[20] the theoretical Weibull slope calculated from the crack-tip stress distribution is about 4. The Weibull slopes

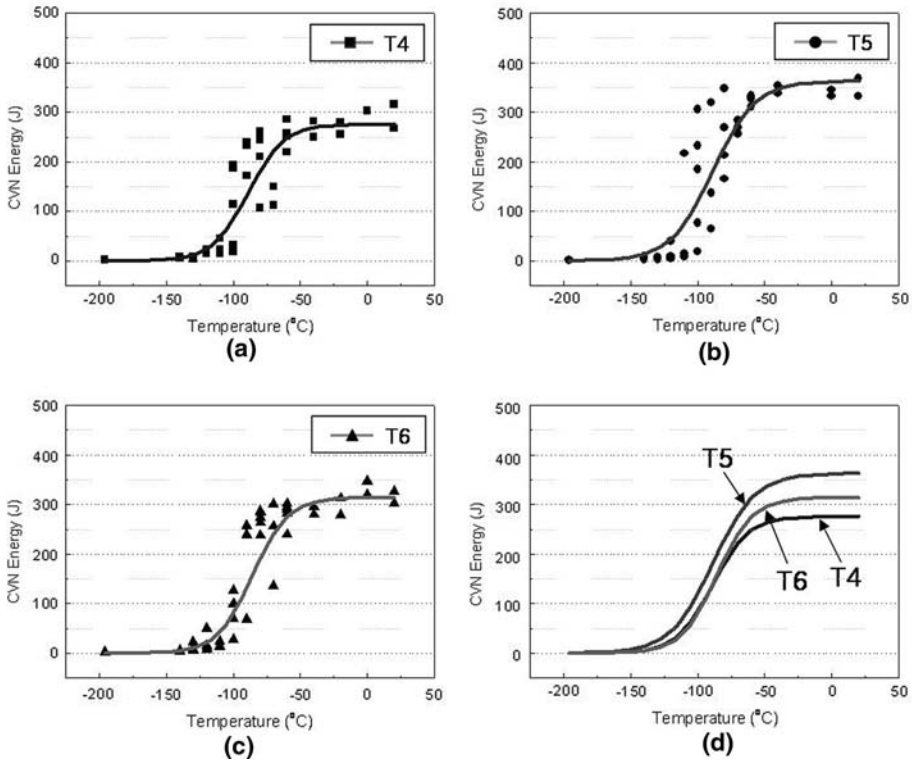

Fig. 6—Variation of Charpy impact energy of the (*a*) T4, (*b*) T5, and (*c*) T6 steels in the temperature range from −196 °C to room temperature. (*d*) Overall impact energy results of the three steels.

Table III. Charpy Impact Test Results

Steel	Upper Shelf Energy (J)	Energy Transition Temp. (°C)	T_{28J} (°C)	T_{41J} (°C)	T_{68J} (°C)
T4	276	−90	−117	−113	−104
T5	363	−89	−127	−123	−112
T6	314	−86	−116	−112	−102

measured on the Weibull plots are nearly consistent with the theoretical slope of 4. In general, the high Weibull slope indicates the small deviation of the fracture toughness data.[8] The Weibull slope measured at −120 °C is higher than that measured at −100 °C, because the deviation of the fracture toughness data decreases with decreasing temperature.

IV. DISCUSSION

The API X70 line pipe steels rolled in the two-phase region have different microstructures, depending on the FCT. The steels consist mostly of PF, together with a small amount of martensite or bainite (Figures 1(a) through (c)). When hard martensite is coarsely distributed in the soft ferrite matrix, as in the T4 steel (Figure 1(a)), a very high stress can be concentrated at martensite/ferrite interfaces because of the difference of the yield strength between the two phases.[21–24] According to Lansillotto *et al.*,[23] the stress is concentrated inside ferrite grains because of the volume expansion during the austenite to martensite transformation, and brittle fracture occurs when this concentrated stress exceeds the fracture stress. In the T4 steel containing martensite, thus, the stress concentration easily occurs at martensite, which can deteriorate the fracture toughness in the transition temperature region. The crack initiation at other brittle areas such as grain boundaries is difficult, because microcracks formed by the dislocation pileup can be readily blunted.[22] Thus, main crack initiation sites in the T4 steel are martensites, at which microcracks form to initiate cleavage fracture.

The SEM micrographs of the cross-sectional area beneath the fracture surface in front of the fatigued precrack of the PCVN specimen tested at −120 °C are shown in Figures 10(a) through (f). In the T4 steel, martensites or martensite/ferrite interfaces are preferentially cracked near the precrack tip, and the initiated microcrack propagates into ferrites (Figures 10(a) and (b)). In the T5 and T6 steels containing bainite, bainites or bainite/ferrite interfaces are preferential microcrack initiation sites (Figures 10(c) through (f)). These results indicate that main fracture initiation sites at which microcracks form to initiate cleavage fracture are martensites and martensite/ferrite interfaces in the T4 steel and bainites and bainite/ferrite interfaces in the T5 and T6 steels.

When the stress is applied in structures containing defects, cleavage cracks initiate first and then propagate to reach the brittle cleavage fracture of the structures. Comparing the three rolled steels in a viewpoint of cleavage crack initiation, cleavage fracture initiates

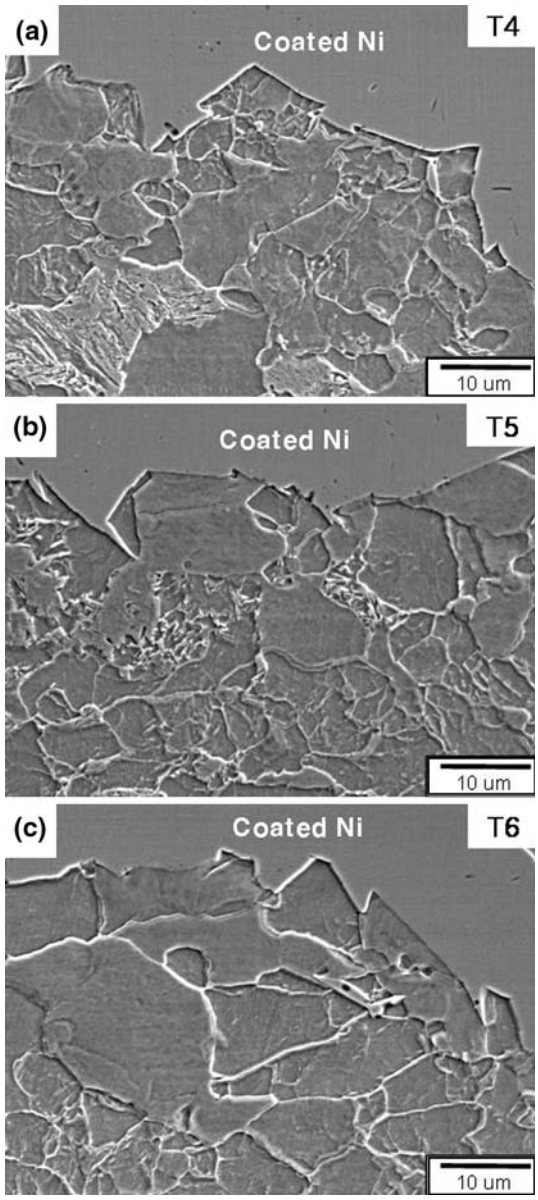

Fig. 7—SEM micrographs of the cross-sectional area beneath the cleavage fracture surface of the Charpy V-notch specimens fractured at −196 °C for the (*a*) T4, (*b*) T5, and (*c*) T6 steels, showing the crack propagation path. Fractured surfaces were coated by nickel.

Table IV. Low-Temperature Tensile Test Results

Steel	Yield Strength (MPa) at −120 °C	Yield Strength (MPa) at −100 °C
T4	683	651
T5	710	655
T6	703	648

more easily in the T4 steel containing martensite than in the T5 steel containing bainite, which has better toughness than martensite.[9,25–27] Thus, the reference temperature (T_o) obtained from the elastic-plastic cleavage fracture toughness test as well as the index temperatures obtained from the Charpy impact test (Table III)

Table V. Fracture Toughness Results at Low Temperatures

	−120 °C		−100 °C	
Steel	$K_{jc(med)}$ (MPa $m^{1/2}$)	T_o (°C)	$K_{jc(med)}$ (MPa $m^{1/2}$)	T_o (°C)
T4	96.1	−97	54.9	−97
T5	105	−104	63.8	−82
T6	96	−97	58	−72

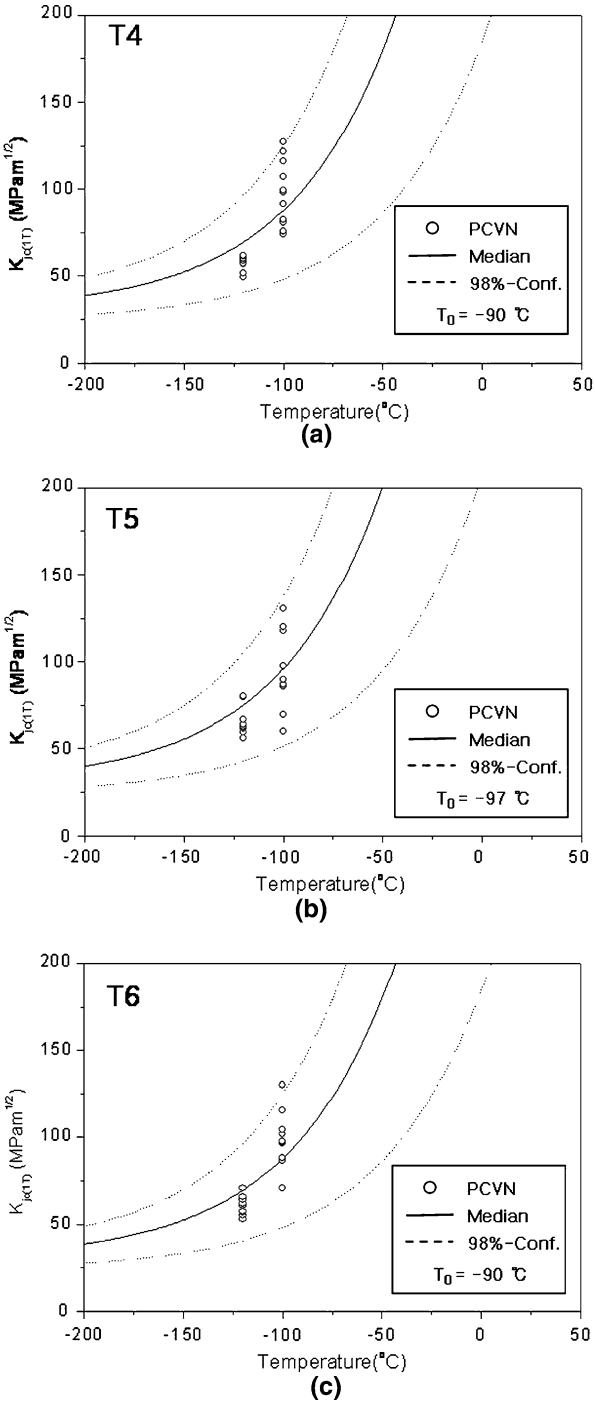

Fig. 8—Master curves and measured K_{Jc} values of the (*a*) T4, (*b*) T5, and (*c*) T6 steels.

Table VI. Uncertainty of the Reference Temperature

Steel	r	β	Z_{95}	ΔT_o(°C)
T4	20	18	2	8
T5	17	18	2	9
T6	19	18	2	8

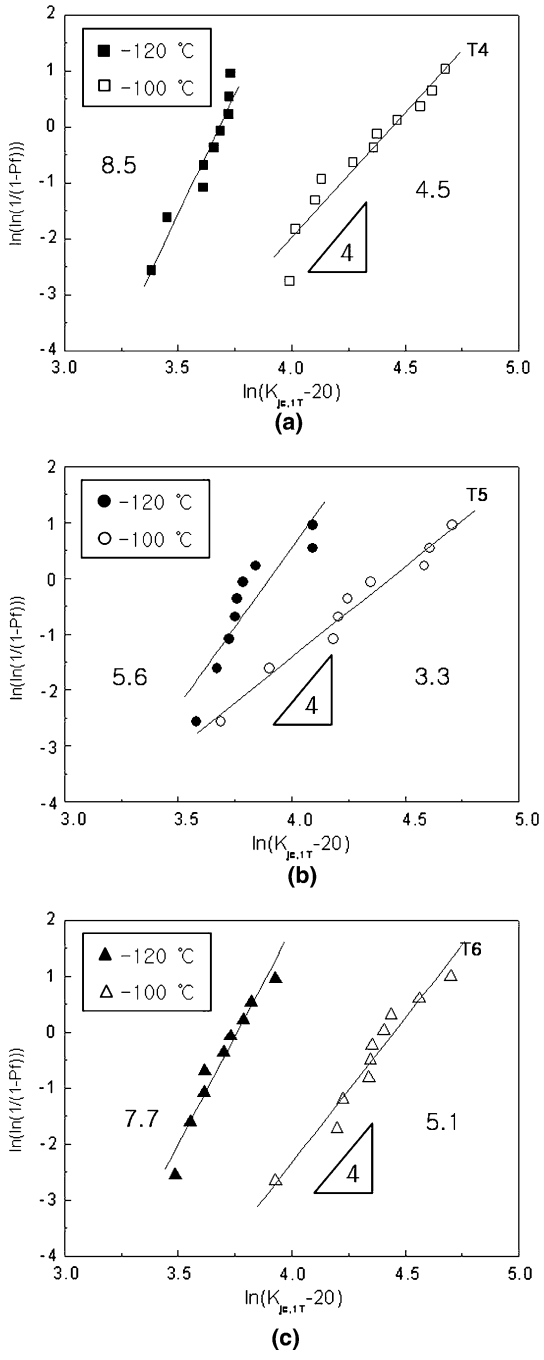

Fig. 9—Statistical distribution of K_{Jc} values determined from the three-parameter Weibull function for the (*a*) T4, (*b*) T5, and (*c*) T6 steels.

are higher in the T4 steel than in the T5 steel. In addition, $K_{Jc(\text{med})}$ values calculated from Eq. [4] are 96 and 105 MPa $m^{1/2}$ for the T4 and T5 steels, respectively. This indicates that the overall fracture toughness in the transition region is worse in the T4 steel, because the T4 steel has the lower $K_{Jc(\text{med})}$ and the higher reference temperature and index temperatures than the T5 steel.

In general, the reference temperature and the index temperatures are well correlated in a linear relationship,[28,29] and this correlation also matches in the T5 and T6 steels having similar microstructure and containing bainite. Comparing the fracture toughness in the transition region of the T5 and T6 steels, the reference temperature and index temperatures are lower in the T5 steel than in the T6 steel. This difference in the transition temperature is largely dependent on grain size and grain boundary misorientation. The transition temperature decreases with decreasing effective grain size as the volume fraction of fine and high-angled (≥15 deg) grains increases. The effective grain size of the T5 steel is smaller than that of the T6 steel (Figures 3(b) and (c)), and its transition temperatures are lower because the T5 steel was fabricated under a faster cooling rate. Considering a viewpoint of cleavage crack propagation, the effective grain size, which can be regarded as the average distance deflecting the cleavage crack propagation path, of the T5 steel is smaller than the T6 steel. Thus, the resistance to the cleavage crack propagation is higher in the T5 steel than in the T6 steel, because the crack propagation in the T5 steel can be effectively blocked. This can also be confirmed from the results of the cleavage crack propagation path of Figures 7(b) and (c). Therefore, the smaller effective grain size positively affects the cleavage crack propagation and improves the low-temperature fracture toughness in the transition region.

The reference temperature of the T4 steel is −90 °C, which is the same as that of the T6 steel. Their index temperatures of T_{28J}, T_{41J}, and T_{68J} are similar, while the ETT is somewhat lower in the T4 steel. These results indicate that overall cleavage fracture properties including fracture toughness and transition temperature are quite similar in both steels, although they are lower than those of the T5 steel. Cleavage fracture initiation is affected by cleavage stress, which is also affected by both the presence of brittle phases such as martensite and the effective grain size. Thus, the presence of martensite in the T4 steel leads to lower resistance to fracture than the T5 steel, and the larger effective grain size in the T6 steel leads to lower resistance to fracture than the T5 steel, thereby resulting in the similar cleavage fracture initiation in both the T4 and T6 steels.

The preceding results indicate that the overall fracture properties of the T5 steel are best because the fracture toughness of the T5 steel is higher than that of the T4 and T6 steels, while the reference temperature and index temperatures of the T5 steel are lower. In the T5 steel, the absence of martensite leads to the higher resistance to cleavage fracture than in the T4 steel, and the smaller effective grain size than that of the T6 steel leads to the higher resistance. In order to improve the fracture toughness in the transition region, thus, it is necessary to minimize or remove martensite and to form a number of fine grains having high-angle grain boundaries.

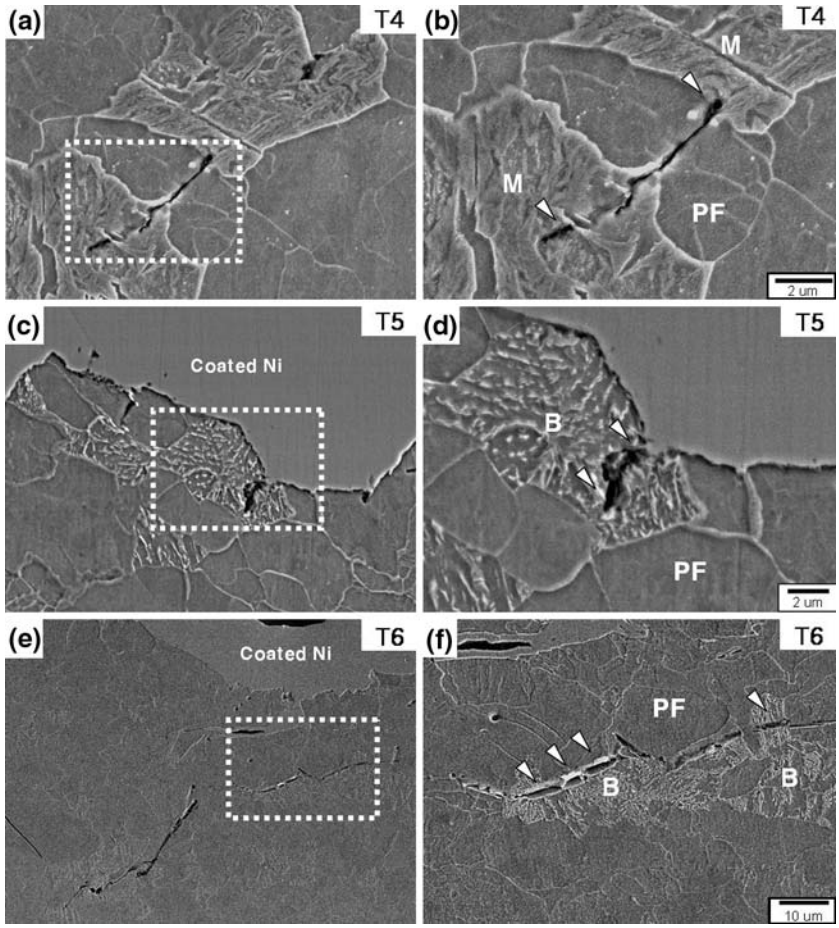

Fig. 10—SEM micrograph of the cross-sectional area beneath the fracture surface in front of the fatigued precrack of the PCVN specimen tested at −120 °C for the (*a*) and (*b*) T4, (*c*) and (*d*) T5, and (*e*) and (*f*) T6 steels, showing the cracking of martensites, martensite/ferrite interfaces, bainites, or bainite/ferrite interfaces. (b), (d), and (f) Higher-magnification SEM micrographs of rectangular areas marked in (a), (c), and (e), respectively. Nital etched.

V. CONCLUSIONS

In this study, fracture toughness in the transition temperature region of the three API X70 line pipe steels was analyzed in accordance with the ASTM E1921-05 standard test method.

1. The fracture toughness test results in the transition region showed that the master curve and the 98 pct confidence curves explained the variation in the measured fracture toughness values well. The Weibull slope measured on the Weibull plots was consistent with the theoretical slope of 4.
2. The reference temperature obtained from the elastic-plastic cleavage fracture toughness test as well as the index temperatures obtained from the Charpy impact test were higher in the T4 steel than in the T5 steel, and the fracture toughness in the transition region of the T4 steel was lower because a considerable amount of martensite, which could act as cleavage crack initiation sites, existed in the PF matrix.
3. The T5 steel had the higher fracture toughness in the transition region and the lower reference temperature and index temperatures than the T4 and T6 steels, because it did not contain brittle martensite and its effective grain size was smaller than that of the T6 steel. The absence of martensite and the smaller effective grain size led to higher resistance to cleavage fracture, thereby resulting in the best overall fracture properties.

ACKNOWLEDGMENTS

This work was financially supported by the National Research Laboratory Program of the Ministry of Science and Technology of Korea. The authors thank Professor Nack J. Kim, Dr. Byoungchul Hwang, and Dr. Young Min Kim, POSTECH, for their help with the fracture toughness testing.

REFERENCES

1. R. Denys: *Pipeline Technology*I-II, Elsevier, Amsterdam, 2000, pp. 1–116.
2. D.P. Fairchild, M.L. Macia, S.D. Papka, C.W. Petersen, J.H. Stevens, S.T. Barbas, N.V. Bangaru, J.Y. Koo, M.J. Luton: *Proc. Int. Pipe Dreamer's Conf.*, M. Toyoda and R. Denys, eds., Yokohama, Japan, 2002, pp. 307–21.

3. K.T. Corbett, R.R. Bowen, and C.W. Petersen: *Int. J. Offshore Polar Eng.*, 2004, vol. 14, pp. 75–80.
4. *API Recommended Practice 5L3*, American Petroleum Institute, API Publishing Service, 1220 L Street, N.W., Washington, D.C. 20005, USA, 1996, pp. 1–8.
5. G. Mannucci and D. Harris: "Fracture Properties of API X100 Gas Pipeline Steels," Final Report, European Commission, Brussels, Belgium, 2002, pp. 1–128.
6. D.J. Horsley: *Eng. Fract. Mech.*, 2003, vol. 70, pp. 547–52.
7. S.-T. Oh, H.-J. Chang, K.H. Oh, and H.N. Han: *Met. Mater. Int.*, 2006, vol. 12, pp. 121–29.
8. *Standard Test Method for Determination of Reference Temperature for Ferritic Steels in the Transition Range*, ASTM Standard E1921-05, ASTM, West Conshohocken, PA, 2005, pp. 1–29.
9. I. Tamura, H. Sekine, T. Tanaka, and C. Ouchi: *Thermomechanical Processing of High-Strength Low-Alloy Steels*, Butterworth & Co., Ltd., London, 1988, pp. 80–100.
10. J.W. Kim, J.W. Choi, and D.B. Bae: *Met. Mater. Int.*, 2005, vol. 11, pp. 131–34.
11. I.D. Choi, D.M. Kim, S.J. Kim, D.M. Bruce, D.K. Matlock, and J.G. Speer: *Met. Mater. Int.*, 2006, vol. 12, pp. 13–19.
12. M. Diaz-Fuentes, A. Iza-Mendia, and I. Gutierrez: *Metall. Mater. Trans. A*, 2003, vol. 34A, pp. 2505–16.
13. *Standard Test Method for Notched Bar Impact Testing of Metallic Materials*, ASTM Standard E23-02, ASTM, West Conshohocken, PA, 2002, pp. 1–27.
14. W. Oldfield: *Curve Fitting Impact Test Data - a Statistical Procedure*, ASTM Standard. News, 1975, pp. 24–29.
15. J.Y. Koo, M.J. Luton, N.V. Bangaru, R.A. Petkovic, D.P. Fairchild, C.W. Petersen, H. Asahi, T. Hara, Y. Terada, M. Sugiyama, H. Tamehiro, Y. Komizo, S. Okaguchi, M. ;Hamada, A. Yamamoto, and I. Takeuchi: *Proc. 13th Int. Offshore and Polar Engineering Conf.*, Honolulu, HI, 2003, pp. 10–18.
16. N.J. Kim: *J. Met.*, 1983, vol. 35, pp. 21–27.
17. B. Hwang, Y.M. Kim, S. Lee, N.J. Kim, and S.S. Ahn: *Metall. Mater. Trans. A*, 2005, vol. 36A, pp. 725–39.
18. Y. Shiota, Y. Tomota, A. Moriai, and T. Kamiyama: *Met. Mater. Int.*, 2005, vol. 11, pp. 371–76.
19. K. Wallin: *Eng. Frac. Mech.*, 1984, vol. 19, pp. 1085–93.
20. T.L. Anderson and D. Stienstra: *J. Test. Eval.*, 1989, vol. 17, pp. 46–53.
21. J.H. Chen, G.Z. Wang, C. Yan, H. Ma, and L. Zhu: *Int. J. Frac.*, 1997, vol. 83, pp. 105–20.
22. G.T. Hahn: *Metall. Trans. A*, 1984, vol. 15A, pp. 947–59.
23. C.A.N. Lanzillotto and F.B. Pickering: *Met. Sci.*, 1982, vol. 16, pp. 371–82.
24. K. Wallin, T. Saario, and K. Törrönen: *Int. J. Frac.*, 1987, vol. 32, pp. 201–10.
25. B.L. Bramfitt and J.G. Speer: *Metall. Trans. A*, 1990, vol. 21A, pp. 817–29.
26. G. Krauss and S.W. Thompson: *ISIJ*, 1995, vol. 35, pp. 937–45.
27. Y.E. Smith, A.P. Coldren, and R.L. Cryderman: *Toward Improved Ductility and Toughness*, Climax Molybdenum Co., Ann Arbor, MI, 1971, pp. 119–42.
28. K. Wallin, K. Törrönen, R. Ahlstrand, B. Timofeev, V. Rybin, V. Nikolaev, and A. Morozov: *Nucl. Eng. Des.*, 1992, vol. 135, pp. 239–46.
29. S. Kim, B. Hwang, and S. Lee: *Metall. Mater. Trans. A*, 2003, vol. 34A, pp. 1275–81.